Clim. Past, 7, 27–39, 2011
www.clim-past.net/7/27/2011/
doi:10.5194/cp-7-27-2011

Climate of the Past

Oceanic tracer and proxy time scales revisited

C. Siberlin and C. Wunsch

Department of Earth, Atmospheric and Planetary Sciences, Massachusetts Institute of Technology, Cambridge MA 02139, USA

Received: 9 August 2010 – Published in Clim. Past Discuss.: 1 September 2010
Revised: 21 December 2010 – Accepted: 3 January 2011 – Published: 11 January 2011

Abstract. Quantifying time-responses of the ocean to tracer input is important to the interpretation of paleodata from sediment cores – because surface-injected tracers do not instantaneously spread throughout the ocean. To obtain insights into the time response, a computationally efficient state-transition matrix method is demonstrated and used to compute successive states of passive tracer concentrations in the global ocean. Times to equilibrium exceed a thousand years for regions of the global ocean outside of the injection and convective areas and concentration gradients give time-lags from hundreds to thousands of years between the Atlantic and Pacific abyss, depending on the injection region and the nature of the boundary conditions employed. Equilibrium times can be much longer than radiocarbon ages – both because the latter are strongly biased towards the youngest fraction of fluid captured in a sample, and because they represent distinct physical properties. Use of different boundary conditions – concentration, or flux – produces varying response times, with the latter depending directly upon pulse duration. With pulses, the sometimes very different transient approach to equilibrium in various parts of the ocean generates event identification problems.

1 Introduction

In a recent paper, Wunsch and Heimbach (2008; hereafter WH08) studied the response of an oceanic general circulation model (GCM) to a passive tracer entering at the sea surface. They sought order of magnitude estimates of the time it takes such tracers to reach equilibrium – a time important to understanding climate change signals appearing in different parts of the ocean. (A passive tracer is one that does not affect the fluid density.) The study was stimulated in part by the paper of Skinner and Shackleton (2005) who described apparent phase delays across Termination I between perceived signals in the abyssal North Atlantic and North Pacific Oceans, and the mechanisms that could account for them. WH08 concluded that the response times for signal propagation from one part of the ocean to another by purely physical means in a quasi-steady ocean circulation were by themselves large enough to produce the apparent delays. Understanding the origin of phase shifts and signal distortion within the ocean is a necessity for the interpretation of possible causes and effects. Lea et al. (2000) is another example of a study in which the apparent time lag between a regional temperature change, and the arrival of the signature of deglaciation, is used to infer a causal link. Of particular concern in the study of deep-sea cores is the oceanic adjustment to the sometimes extremely strong signature of changes in ice volume entering the ocean as a freshwater flux carrying e.g., δ^{18}O, signatures that eventually influence the entire ocean.

The idealized study of the behavior of tracer introductions into the ocean circulation also raised a second important factor: to what extent do major transient structures, e.g. step-like shifts in concentration or flux, forced at the sea surface, survive at depth so that the time histories recorded in the abyssal ocean replicate the structures imposed at the sea surface? That is, posing a specific question: if there is an abrupt pulse-like transient in the introduction of a proxy such as δ^{18}O in the high latitude North Atlantic, do the sediments of the Pacific Ocean record that same pulse-like transient – thus rendering mutual identification easy? Or is the Pacific record so transformed by passage through the ocean that the matching of events is problematic? These questions need to be answered before e.g., using the records to make inferences about whether and how the circulation itself changed – and changes are inevitable under climate shifts.

Correspondence to: C. Wunsch
(cwunsch@mit.edu)

Published by Copernicus Publications on behalf of the European Geosciences Union.

Although the intention of WH08 was simply to gain an understanding of the time scales present in the oceanic adjustment process to tracer input, their inferences were subsequently criticized by Primeau and Deleersnijder (2009; hereafter PD09). WH08 relied upon a concentration boundary condition (Dirichlet), and PD09 pointed out that either a surface *flux* (Neumann) or mixed (Robin) boundary condition would be more natural. For many of the proxies of paleoceanographic interest, there is little doubt that surface flux rather than surface concentration boundary conditions are more appropriate and PD09 concluded that equilibrium times would then be shorter. It is also apparent, however, that such boundary conditions can lead to *longer* adjustment times – as we will discuss – and that studies of equilibrium under such circumstances are necessarily somewhat more complex.

Both WH08 and the present paper should be regarded as elaborated version of the fluid dynamicists' scaling studies: directed at understanding basic time and space scales of the entry of proxies into the ocean. The resulting orders of magnitude provide a foundation for the interpretation of the far more complex details of real records and the real ocean.

A considerable literature has grown up in recent years around the general, mainly theoretical, problems of the interpretation of tracer data. Much of the focus of that literature (see e.g., Waugh et al., 2003, for many earlier references), has been in the context of what are labelled "travel time distributions" in which the distribution of water mass origins at different points are treated as though they are stochastic variables derived from a probability density (the travel time distribution). That point of view is an interesting one, but implies an underlying stochastic physics distinct from any deterministic quasi-steady-state. In practice, "travel time distributions" are known to a much broader community as Green function solutions – a standard, deterministic, methodology for solution of partial differential equations. PD09 discuss the approach to equilibrium distributions in terms of eigensolutions to the governing models. This, too, is an interesting and enlightening methodology. Although these and other methods can be helpful (some of them are very powerful tools in analyzing *model* calculations of tracers), it is not so obvious that the use of real tracers in paleoceanography is rendered easier by their employ. Because of the importance of proxy tracers in paleoclimate, and in keeping with the purpose of WH08 as providing a semi-quantitative guide to interpreting tracers, it is worthwhile revisiting this subject to summarize those inferences that are likely to be robust. Much of what is here derives from the recent thesis of Siberlin (2010) and is intended in part as a tutorial: theories of tracer inferences are scattered through a not-always-transparent technical literature. We endeavor to employ as little mathematics as is practical, and some of the details have been put into Appendix A.

For context, consider a global ocean of volume, V. It is supposed that the three dimensional water circulation within V is known (it can be time-dependent) as are any mixing coefficients. A passive tracer, C (one not affecting the water density or its dynamical properties), is introduced at the sea surface of the volume, and supposed to satisfy a conventional advection-diffusion equation of the form,

$$\frac{\partial C}{\partial t} + \mathbf{v}\cdot\nabla C - \nabla\cdot(\mathbf{K}\nabla C) = q, \tag{1}$$

where $\mathbf{v}(\mathbf{r},t) = [u,v,w]$ is the three-dimensional flow field, $\mathbf{K}$ is a mixing tensor, and q represents interior sources or sinks including, where appropriate, decay terms such as $q = -\lambda C$ as in ^{14}C. ∇ is the three-dimensional gradient operator, $\nabla = [\partial/\partial x, \partial/\partial y, \partial/\partial z]$ (in practice, one uses spherical coordinates). $\mathbf{r} = [x,y,z]$ is a generic position vector. (Observed isotopic *ratios*, such as used for neodymium, Nd, do not satisfy this equation: instead the numerator and denominator separately satisfy one like it, with the ratio itself being described by a complex non-linear relationship; e.g. Jenkins, 1980).

Ages

Most of the paleotracer community has relied not upon equilibrium times as discussed by WH08, but upon radiocarbon ages, which in general prove considerably shorter. The use of radiocarbon introduces the entire complex subject of "age" tracers in various definitions and interpretations. Gebbie and Huybers (2010b) provide an overview and many earlier references. For the moment, consider only the very simple case of a water sample, perhaps one in the deep South Pacific, made up of N fluid parcels of equal volume which left the sea surface at a variety of times, t_i, before forming the measured sample. In the transit time distribution point of view, the t_i are selected from a probability density function, but as already noted, this interpretation is not a necessary one, and here they are regarded as values fixed at any observation point. For maximum simplicity, assume further that the surface starting concentration of radiocarbon is identical, C_0, in all components, and that there is no exchange by diffusion or other process along the pathway to the observation location. Then the radiocarbon concentration, when measured, is

$$C_{obs} = \frac{1}{N}\left(C_0 e^{-\lambda t_1} + C_0 e^{-\lambda t_2} + \ldots + C_0 e^{-\lambda t_N}\right),$$

where $\lambda \approx 1/8267$y is the radiocarbon decay constant (half-life 5730y). The true mean age, $\bar{\tau}$, would be the ordinary average of the arrival times,

$$\bar{\tau} = \frac{1}{N}\sum_{i=1}^{N} t_i. \tag{2}$$

The radiocarbon age is

$$\tau_{RC} = -\frac{1}{\lambda}\ln\left(\frac{C_{obs}}{C_0}\right) = -\frac{1}{\lambda}\ln\left[\left(e^{-\lambda t_1} + \ldots + e^{-\lambda t_N}\right)/N\right],$$

where the t_i are the increasing lag times. If there is only one time of arrival, $\tau_{RC} = \bar{\tau}$. With two arrivals, $\tau_{RC} < \bar{\tau}$, because $\exp(-\lambda t_2) < \exp(-\lambda t_1)$. The radiocarbon age is biassed, perhaps strongly so, towards the age of the most recent arrival – concentrations from longer elapsed-time arrivals giving strongly down-weighted contributions. If the second arrival took much longer than the radiocarbon decay time, so that $C_0 \exp(-\lambda t_2) \approx 0$, then $\tau_{RC} = t_1$ and the potential difference between the mean age, $\bar{\tau} = (t_1 + t_2)/2$ and the radiocarbon age is potentially very large. Various simple examples of this bias error can be worked out from assumptions about travel time values (see the references), but which we do not pursue here. In this same situation, one can define the approach to equilibrium for a stable tracer by noting that if fluid arrives N-times at the observation point with equal fractional contributions, where the initial concentration is $C = 0$, then it will rise toward its final concentration of C_0 asymptotically as the different water parcels appear, the full value being obtained only after the last contribution has arrived. If, following WH08, effective equilibrium is arbitrarily defined as the time when $C(t) = 0.9C_0$, then t_{90} will always exceed $\bar{\tau}$, the mean time, and $\bar{\tau}$ will always exceed τ_{RC}. (Equilibrium times are discussed further below.) This bias is well known in the context of numerical model "ideal tracer ages" (e.g., Khatiwala et al., 2001). The degree of bias, and hence the apparent age, depends upon λ, and so is a property of the tracer and not just the fluid.

The main message is that, *assuming the initial surface values of C are not greatly different*, one expects calculated tracer ages to be systematically less than mean ages, sometimes greatly so, and that they can prove considerably shorter than equilibrium times, is no particular surprise. If the values of the t_i were known, as they can be in a numerical model, the bias can be corrected. But with isolated radiocarbon data alone, it is not possible. The investigator using these ages must be clear on the physical meaning of the different ages and the context in which they are being employed. WH08 used equilibrium times because tracer concentrations appear in Eq. (1) as spatial and temporal gradients; the use of disequilibrium values in a steady-state can introduce major errors and produce misleading inferences about travel time differences of tracer anomalies, or rates of biological productivity or remineralization. Equilibrium times, mean ages, and tracer ages define different physical variables and cannot be simply interchanged.

Radiocarbon ages are generally lower bounds on the mean ages of water parcels (see Gebbie and Huybers, 2010b), and methods for getting beyond that – outside of numerical models where complete calculations are possible – are not so obvious. The situation would be much more extreme for shorter-lived isotopes such as tritium. (See Gebbie and Huybers, 2010b for further discussion and references.) If two water parcels produce radiocarbon ages in which one is younger than the other, little can be inferred directly about the time-mean age. Because water parcels will not travel unchanged from the surface, but will exchange diffusively with their surroundings along potentially very long trajectories, the real situation is actually far more complex. Radiocarbon ages will be discussed a bit more below.

Time scales

Tracer problems in three-dimensions, satisfying equations such as Eq. (1), produce a multiplicity of time scales and which can and will appear in the solutions and, depending upon their magnitudes, determine the structure of the oceanic response. Let the volume, V, under consideration have cross-section L, and depth D. If one assumes, for maximum simplicity, that $\mathbf{K}$ is composed solely of constant diffusion coefficients K_z in the vertical and K_x in the horizontal, then out of the equation one can construct numerous time scales (see e.g., Wunsch, 2002) including, $T_1 = D^2/K_z$, $T_2 = L^2/K_x$, $T_3 = D/w$, $T_4 = 1/\lambda$, (there are others). Mathematically, the final equilibrium of an advection-diffusion process, as in Eq. (1), is always controlled by the diffusive terms, which ultimately erase the strong gradients sometimes generated by the advective ones. In any complete solution to Eq. (1), one expects *all* of these timescales to appear. Whether they are of any practical significance to someone interpreting that solution depends upon the problem details. If the tracer were tritium, with a half-life of about 12 years, injected into the North Atlantic alone, the solution in the deep North Pacific would include terms involving $T_2 \approx 2000$ years. But as the concentration in the deep Pacific would always be vanishingly small, T_2 would be irrelevant in practice. If the tracer were, however, ^{14}C, with a half-life of about 5730 years, the longest of the internal time scales T_i would likely be of concern. In general these time scales are $e-$folding times, representing achievement of about 65% of any final value.

WH08 took a modern ocean circulation estimate derived from a least-squares fit of a general circulation model (GCM) to 14 years of global oceanic data sets, and ran it in a perpetual loop for about 1900 years. Tracers were introduced in a series of numerical experiments to determine time scales in which near-equilibrium could be obtained. That is, a concentration of $C = 1$ (conceptually, a red "dye,") was introduced at the sea surface at time $t = 0$, in one instance over the entire surface area, B, of the global ocean, and held fixed. In other experiments, tracer was introduced into a sub-area, B_1, such as the northern North Pacific or North Atlantic and held fixed. In the remaining, undyed, surface area, a condition of no flux to the atmosphere was imposed. The purpose of this latter requirement was to prevent dye from being exchanged with the atmosphere outside of the input region so that all of it remained within the ocean. With the dye thus being conserved in the ocean, one could then infer, without actually computing it, that the final equilibrium state would be a globally uniform value of $C = 1$ everywhere in a steady-state (the entire ocean ultimately would be dyed red).

Although no analytical solution to Eq. (1) is available, one expects all of the adjustment times, T_i, to be present at every location in the ocean, with a solution structure in which different regions would be dominated by one or more, but differing, time scales. For example, in a solution in which the dye was introduced only in the northern North Atlantic, one might expect that below the surface there, in a region of Ekman downwelling, that the solution would be controlled by D/w, in a potentially very rapid response. In contrast, for the same solution in a region of Ekman upwelling, the main time scale might be the diffusive one, D^2/K_z. In the remote Pacific, the dominant time scale could be horizontal diffusion, L^2/K_x. To provide a simple diagnostic of the many time scales, WH08 used the "90% equilibrium time", t_{90}, as a measure of the time to equilibrium. That is, with the knowledge that the final steady-state is $C = 1$, always reached from below, one could map the time when 90% of this value was obtained in the solution.

As they discuss, however, the time to full equilibrium is formally infinite, and the choice of t_{90} is largely arbitrary: the appropriate value depends upon one's goals. In more complex boundary value problems, the final equilibrium concentration, $C_\infty(\mathbf{r})$, will not be uniform, and one might seek to map its values for substitution into a steady version of an equation such as (1) for the purpose e.g., of determining, K_z. A 10% error in the true equilibrium value might be tolerable, while a different error might be acceptable if e.g., the problem is determining the global inventory of C at equilibrium. For some other problems, one might require the time of first arrival of measurable tracer at a distant location as a measure of a "signal velocity". Such a use evidently depends upon the measurement capability translated into a detection threshold. A similar dependence upon measurement accuracies and precisions could dictate a different equilibrium level determination. That is, if measurement technology cannot distinguish between $C = 0.9$ and $C = 1$, there would be little point in using t_{98}. L. Skinner (personal communication, 2010) has suggested that the equivalent of t_{50} is conventionally used in the paleoceanographic community. While perhaps no more arbitrary than a choice of t_{90}, any attempt to estimate the different terms of Eq. (1) from t_{50} concentrations, will incur errors of order 100%.

Additional, practically important, time scales are those imposed by the boundary data – e.g., the time duration of a pulse of tracer and/or whether it is strongly seasonal – be it from a concentration or flux boundary conditions. Whether the boundary conditions or the circulation remain steady-enough to render useful a discussion of equilibrium can only be decided on a case-by-case basis.

2 External time scales

The WH08 solutions depend only upon the *internal* time scales, T_i, of the problem. In the pulse injection solutions of PD09, an *external* time scale, T_{ext}, was necessarily introduced. That is, if dye is injected at a fixed rate, rather than imposed as fixed surface concentration, and if it is similarly conserved within the ocean, there is no final steady equilibrium. Instead, the final state would be a growing concentration,

$$C(\mathbf{r},t) \sim M(\mathbf{r})t, \tag{3}$$

where $M(\mathbf{r})$ is a complicated function of position. To avoid this situation, PD09 define T_{ext} such that,

$$T_{\text{ext}} F_0 B_1 = C_\infty V,$$

where F_0 is the rate of injection, B_1 is the area of injection, and $C_\infty = 1$. That is, given F_0, T_{ext} is chosen so that the total amount of injected dye is exactly that value producing a total final ocean concentration of $C = 1$ uniformly everywhere – as before. Once again, the final concentration, when reached, will be uniform and the total injected dye will be the same as obtained from the concentration boundary conditions of WH08.

That such a pulse can lead to a rather different temporal behavior is readily seen by choosing $T_{\text{ext}} = 1$ year. All of the dye comes in e.g., in the North Atlantic, in one year (perhaps by a glacial ice-melt event). Such an injected pulse will build up very large concentrations in the North Atlantic in such a way that in and near that region, all of the terms of Eq. (1) involving spatial derivatives such as $\partial C/\partial y$, $\partial^2 C/\partial z^2$, can become extremely large, and hence greatly increasing regional values of $\partial C/\partial t$. Regionally, the time to reach $C = 1$ can be extremely small (albeit the space-time history, as shown below, is sometimes complex – involving overshoots of the final concentration value). It is this increase in regional derivatives that underlies the shortened timescales seen by PD09. Note that in the concentration problem of WH08, the value of C nowhere ever exceeds $C = 1$, and thus the spatial differences of C are clearly bounded by $(C = 1) - (C = 0) = 1$, while no such bound applies in the flux case. (A dependence upon area, B_1, is also present, but that will not be explored here.)

On the other hand, the same logic can lead to a much increased adjustment time. If the same amount of dye is introduced over 1000 years, rather than 1 year, the maximum regional concentrations will be 0.1% of those implied by the one-year pulse, and the rates of change of C proportionally smaller.

3 Some illustrative experiments

As the purpose of this paper is to provide some further insight into the evolution of proxy tracers, it is helpful to explore some solutions under a variety of boundary conditions, including those of WH08 and PD09. Calculation over thousands of years in a realistic ocean circulation of tracers obeying equations such as (1) remains computationally challenging. WH08 used a so-called online version of the full GCM

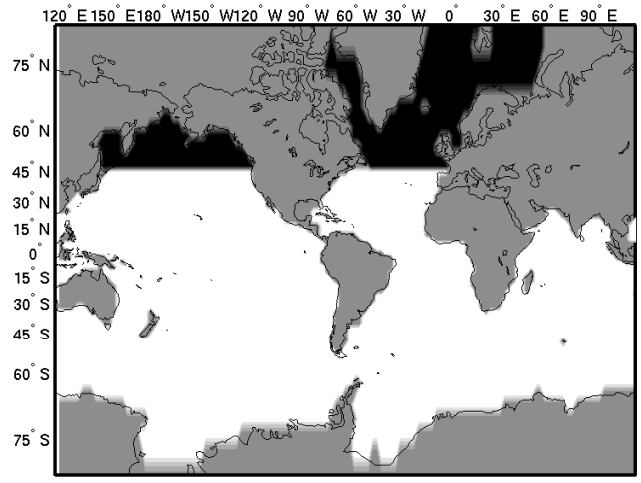

Fig. 1. The two injection regions discussed here, the North Atlantic and the North Pacific, but always employed separately.

code and limited themselves to 1900 years – exploiting their knowledge of the final equilibrium state. Here we use an efficient numerical scheme made possible by the so-called state transition matrix determined for the same GCM by Khatiwala et al. (2005) and Khatiwala (2007). Some additional approximations are made using this form, and so one chore is to demonstrate that solutions do not qualitatively differ from those of WH08 (orders of magnitude effects still being the focus).

3.1 The state transition matrix

Eq. (1) is a linear system and (e.g., Brogan, 1991, Wunsch, 2006) it can be written, very generally, in so-called state vector form,

$$\mathbf{x}(t+\Delta t) = \mathbf{A}(t)\mathbf{x}(t) + \mathbf{B}\mathbf{q}(t), \tag{4}$$

where $\mathbf{x}(t)$, the state-vector, is the vector of concentrations at every grid point at discrete time, t. The "state transition matrix," $\mathbf{A}(t)$, can be derived from the GCM code normally used to calculate $C(t)$ (Khatiwala et al., 2005, and others, discussing transit time distributions, usually call it the "transport matrix;" we prefer our more generic terminology – which is widely used in the control literature. Note also that in oceanography, "transport" is often assumed to denote, specifically, the advective component, not including the diffusive part.) $\mathbf{B}\mathbf{q}(t)$ is, in the notation of Wunsch (2006), a general representation of the boundary conditions and sources. The representation is applicable, by increasing the state vector dimension, for models using implicit calculations (e.g., Siberlin, 2010), as written out in Eq. (3) of Khatiwala (2007). For large time, often $\mathbf{B}\mathbf{q}(t) \rightarrow \mathbf{B}\mathbf{q}_\infty$, a constant vector. Suppose that this system is time-stepped until a steady-state is reached. Then,

$$\mathbf{x}(t+\Delta t) = \mathbf{x}(t) = \mathbf{x}_\infty \tag{5}$$

and it must be true from Eq. (4), that

$$\mathbf{x}_\infty = \mathbf{A}(t)\mathbf{x}_\infty + \mathbf{B}\mathbf{q}_\infty \tag{6}$$

If a steady-state does emerge, the time variations in $\mathbf{A}(t)$ must become sufficiently small that it too can be treated as a constant, $\mathbf{A}_\infty$. Then it follows immediately (e.g., Brogan, 1991, Wunsch, 2006),

$$\mathbf{x}_\infty = (\mathbf{I} - \mathbf{A}_\infty)^{-1}\mathbf{B}\mathbf{q}_\infty. \tag{7}$$

That is, the final, asymptotic state can be computed through the inversion of a single, very sparse, matrix (equivalently, from the solution of a very sparse set of simultaneous equations). Although the matrix is available at climatological monthly intervals, for present purposes its annual mean value is used. That approximation removes some of the physics of wintertime convection, and it is necessary to confirm that, among other approximations, it does not greatly modify the time scales. (Forward-in-time tracer concentration calculations are usually numerically stable and the matrix inverse will exist. In any case, generalized inverses (Wunsch, 2006) could be used if they ever proved necessary.)

Although it is not the primary interest here, it is useful to briefly explore steady-states more structured than the simple one used by WH08. Thus, we exploit the availability of the state transition matrix provided to us by S. Khatiwala (private communication, 2009, 2010). $\mathbf{A}$ is found by computing numerical Green function solutions from a 2.8° horizontal resolution, 15-vertical layer, configuration of the MITgcm with a 20 min time-step, and forced with monthly mean climatological fluxes of momentum, heat and freshwater. Some additional model details are provided in Appendix A. Consider, by way of example, a system in which a large North Atlantic region (see Fig. 1) is dyed (a concentration boundary condition held fixed), but with the initial concentration set to $C = 0$ everywhere else. (This boundary condition permits an exchange of tracer with the atmosphere so as to maintain the values imposed.) The final steady-state concentration is no longer uniform (see Fig. 2). This use of the state transition matrix, with any boundary condition, would be important in helping to interpret tracers believed at equilibrium.

In addition, using $\mathbf{A}$, the time stepping solutions of Eq. (4) can also be obtained very rapidly. The goal remains the same as in WH08: to obtain order of magnitude estimates of the time required for a passive tracer to come close to equilibrium under transient forcing. We emphasize that solution details are not the focus of attention, as it would be difficult to defend a circulation remaining fixed over thousands of years. As stated above, one should regard the results that follow as a scale analysis of the ocean circulation, one believed semi-quantitatively correct, and so useful as a guideline in interpreting proxy and other tracer data.

Although a variety of experiments is discussed by Siberlin (2010), we confine this discussion to a subset involving inputs restricted to the North Atlantic and North Pacific. It

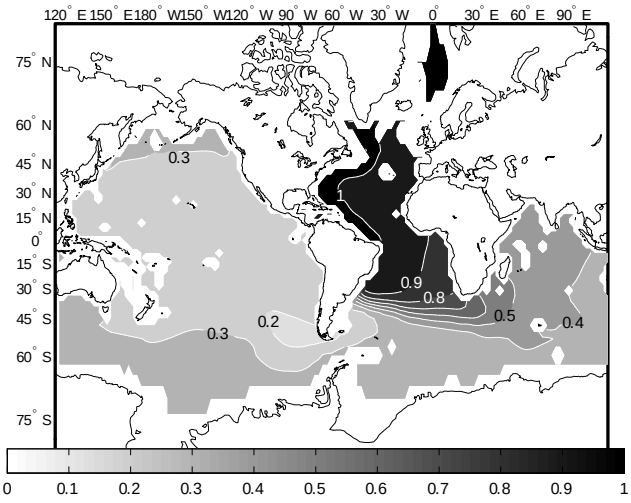

Fig. 2. Steady-state (equilibrium) concentration at 2030m from the concentration (Dirichlet) surface boundary conditions, $C = 1$ held fixed in the North Atlantic, and with $C = 0$ outside that area.

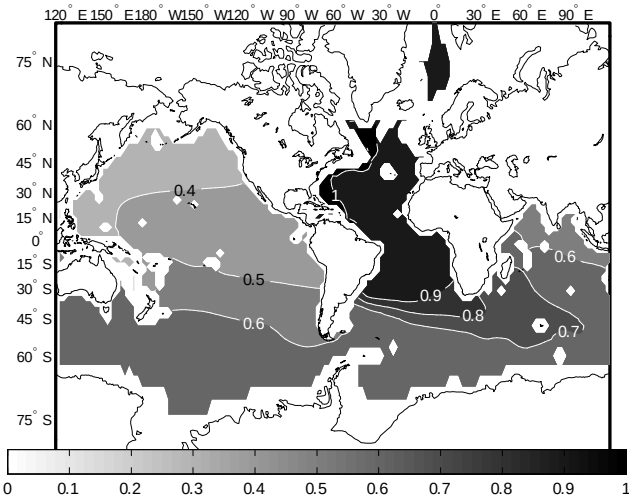

Fig. 3. Tracer concentration after 2000 years at 2030 m from a Dirichlet-Heaviside injection confined to the North Atlantic with no flux elsewhere. Strong spatial gradients persist in a situation where the final equilibrium is uniform, $C = 1$, everywhere.

proves convenient to discuss three distinct boundary conditions: (1) Concentration-step (Dirichlet-Heaviside) in which the concentration at the sea surface is fixed at $C = 1$ and held there indefinitely. Outside this region, there is no atmospheric flux, thus conserving total tracer entering the ocean (WH08). (2) Flux-step (Neumann-Heaviside) in which a flux boundary condition is imposed in some region and held there indefinitely. No tracer transfer back to the atmosphere is permitted anywhere and no steady state exists. (3) Flux-pulse (Neumann-pulse) in which the flux of (2) is re-set to zero after $t = T_{\text{ext}}$, and where the total injected tracer is identical to that in (1) after infinite time (PD09). We will not discuss the mixed-boundary condition (Robin), but see PD09. Because of the complexity of the connections between surface exposure and the ultimate pathways of fluid parcels (see Gebbie and Huybers, 2010a) solutions can be sensitive to precisely where dye is introduced, by any of the boundary conditions. Note, in particular, that dye can be introduced *anywhere* in the ocean, and with these boundary conditions, the ultimate equilibrium is always a uniform oceanic distribution. Input areas here are, for illustrative purposes, very large – occupying essentially all of the subpolar gyres. In practice, melting ice and freshwater enter the ocean at the edges, and the subsequent trajectories will be quite complicated, involving strong boundary current exports, and mixing, and unlikely to occupy such large surface areas within basins. Accurate calculations require *much* higher model resolution to find dye trajectories. We thus err here on the side of more massive forcing than is likely – a forcing that will shorten apparent times to equilibrium.

3.2 North atlantic injection

The high latitude North Atlantic is of particular interest because it has the most rapid communication with the abyss through the winter-time convection processes, but also because it would be one of the major regions of injection of glacial water melt, producing anomalies in tracers such as δ^{18}O. In that region, only a few decades are required in the present calculation to achieve *local* equilibrium at the bottom of the ocean, which is faster than the centuries required by WH08. The most plausible explanation is the coarser resolution of the present model (2.8° as compared to 1°), which tends to convect more rapidly.

The dye convects to great depths at high latitude and is carried to the south by the North Atlantic Deep Water (NADW) on the western boundary. After reaching the Southern Ocean, some dye is upwelled, entering the Antarctic Circumpolar Current (ACC). Then, some advects and diffuses near-bottom into the Pacific and Indian Oceans and there it is diffused vertically and further upwelled. Figure 3 depicts the concentration at 2000 m after 2000 years for a concentration-step $C = 1$ applied in the North Atlantic. Observe that the North Atlantic is at equilibrium ($C > 90\%$), the Southern Ocean is at $C \approx 70\%$, and the Pacific Ocean is at $C \approx 40\%$ of their final values. The mid-depth Pacific, as expected, takes the longest to reach equilibrium.

Figure 4 shows the evolution of the dye average concentration in three regions of the ocean from the North Atlantic concentration step. Qualitatively, with this boundary condition, the rise toward equilibrium from below is globally similar. The time-lag of 4000 years between the bottom of the Atlantic and Pacific is consistent with WH08.

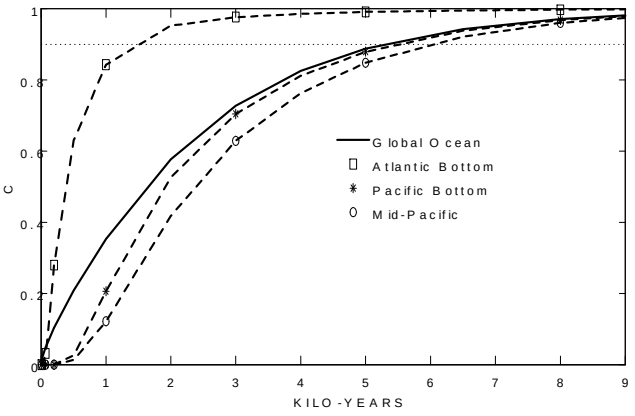

Fig. 4. Concentration averaged over the global ocean and at selected areas (bottom of the North Tropical Atlantic, bottom of the North Tropical Pacific and Mid-Pacific) from an injection confined in the North Atlantic. Ultimate equilibrium is $C = 1$ everywhere. Note the large difference in the times to approach t_{50} and t_{90}.

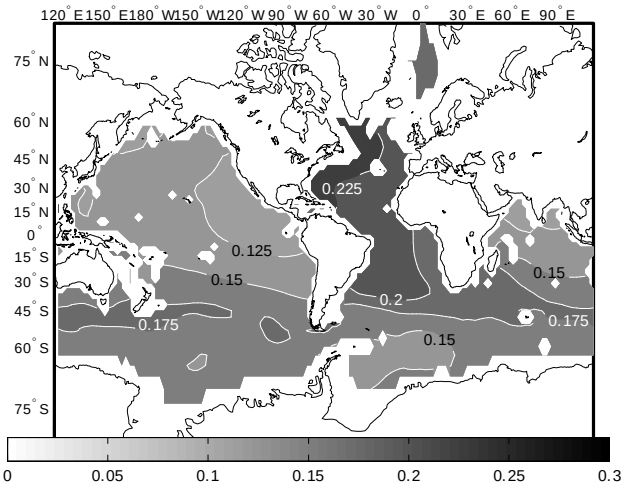

Fig. 5. Tracer concentration after 2000 years at 2030 m from Dirichlet boundary conditions confined to the North Pacific. Despite the local input, the Pacific values are lower than the North Atlantic ones. Again, final equilibrium would be $C = 1$ uniformly.

3.3 North pacific injection

A concentration-step applied in the North Pacific Ocean north of 45° N provides a useful comparison to the injection of tracer in an area of deep water formation. Here, the dye sinks in the North Pacific and stabilizes near 1000 m. It is advected to the south by the subtropical gyre, crossing the basin zonally to the west, being carried by the North Equatorial Current and driven further to the south into the Indian Ocean through the Indonesian Passages, a route which was also noted by WH08. Carried eastward by the ACC, the dye is moved into the Atlantic Ocean by the surface currents – to the West African coast first – where the model Benguela Current operates, then zonally at the latitude of the South Equatorial current and finally northward in the model Gulf Stream. When reaching the Atlantic northern boundary, it is carried convectively downward and then advected south again within the NADW.

Figure 5 shows the concentration at 2000 m after 2000 years for concentration-step, $C = 1$, in the North Pacific region. Even with North Pacific injection, the mid-depth Pacific takes the longest time to reach equilibrium, which is again consistent with WH08. Note that in the modern world, there is a significant Arctic Basin flow of order 1 Sv between the North Pacific and the North Atlantic, which could make the times to equilibrium smaller in this critical area – by shortening the time necessary to transfer the dye at the Pacific surface to a region of deep convection (the North Atlantic); WH08. The present configuration is perhaps more suitable for the Last Glacial Maximum with a closed Bering Strait. Figure 6 shows the evolution of the average dye concentration in three regions from the North Pacific concentration step. All regions remain far from equilibrium after 10 000 years. The bottom of the tropical Atlantic barely reaches 50% of its final concentration after 7000 years, with the Pacific further behind (the bottom of the tropical Pacific reaches 50% of its final concentration after 8000 years).

3.4 Dirichlet and neumann boundary conditions

The time histories in the North Atlantic and North Pacific are different and depend on the injection region. The paths taken by the dye for the three boundary conditions – concentration-step, flux-step, flux-pulse – are similar, but the time-scales on which the equilibrium is achieved are drastically different.

Figures 7 and 8 depict the evolution of concentration in three different regions of the ocean, when a Neumann flux-pulse is imposed in the North Atlantic and the North Pacific for two external time-scales T_{ext}: a pulse of 1 year ($T_{\text{ext}} = 1$y) and of 1000 years ($T_{\text{ext}} = 1000$y). The overshoots in concentration beyond $C = 1$ are the consequence of the initial high concentrations at the surface. For $T_{\text{ext}} = 1$, t_{90} is shorter than in the concentration-step experiments. The time lag Δt_{90} (the time difference between the Pacific and Atlantic bottom reaching 90% of its final value) is also shorter than the 4000-year delay observed in the Dirichlet-Heaviside North Atlantic experiment (as in PD09). Here all the dye has been introduced in the ocean after a year and is then homogenized by advection and diffusion processes. In the Dirichlet experiment however, the concentration boundary condition prescribed implies a flux between the surface patch and the waters underneath that is time-dependent: the tracer gradient normal to the patch depends on the rate at which waters are moving away from the patch (PD09). This gradient will decrease with time, as the ocean is moving toward uniform dye concentration. When the $T_{\text{ext}} = 1000$ years, t_{90} and Δt_{90} increase as well. Even with a 1000-year pulse, the

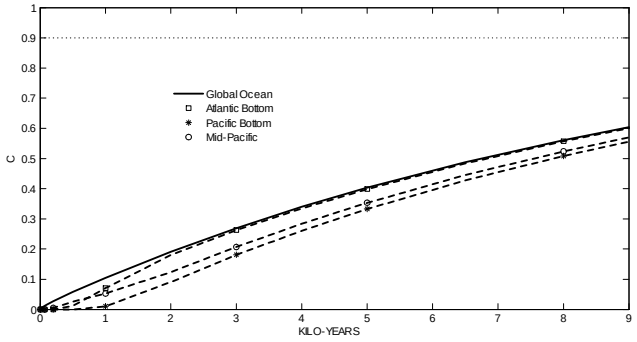

Fig. 6. Concentration averaged over the global ocean and at selected areas (bottom of the North Tropical Atlantic, bottom of the North Tropical Pacific and Mid-Pacific) from a Dirichlet-Heaviside injection confined in the North Pacific. Ultimate equilibrium is $C = 1$ everywhere.

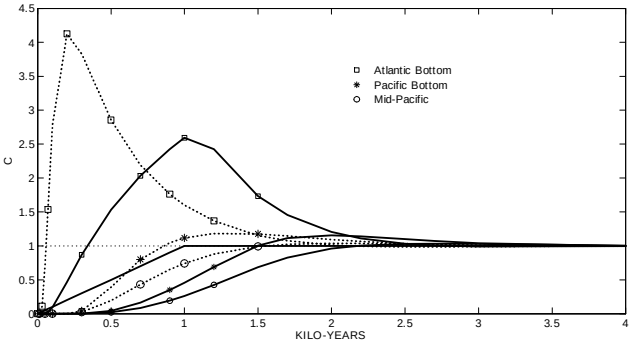

Fig. 7. Concentration averaged over the global ocean and at selected areas (bottom of the North Tropical Atlantic, bottom of the North Tropical Pacific and Mid-Pacific) from a Dirichlet-Heaviside injection confined in the North Pacific. Ultimate equilibrium is $C = 1$ everywhere.

resulting concentration at the surface can reach $C = 200$ because the dye accumulating in those areas leads to large interior derivatives, and at least a regional acceleration toward local equilibrium.

These figures make a general, important, point – what appears pulse-like in one part of the ocean is transformed by the fluid physics into a quite different time-dependent signal farther away. Diffusion, which will be acting over several thousands of years, removes the short space and time scales necessary to produce step- or pulse-like behavior, thus transforming abrupt shifts, usually on short spatial scales, into much more gradual ones on large space scales. Distortion of transients as they move through the advecting and diffusing ocean is both qualitatively and quantitatively important, and interpreting what might be recorded in the sediments can only be done with knowledge of the transformation process. This process will produce differing results depending upon, among other elements, whether injection is local or global. Appendix B shows an analytical example of the change from a pulse to a distorted rise in a one-dimensional, purely diffusive system. (Although de-emphasized here, solutions to advection-diffusion problems display a large variety of space scales, as well as of time scales.)

3.5 Decaying tracer

The impact of a decay constant on tracer ages has been extensively studied both theoretically and numerically (e.g., Khatiwala et al., 2001, 2007; Waugh et al., 2002, 2003; Gebbie and Huybers, 2010b). "Tracer age" is usually defined as the elapsed time since the tracer was injected into the flow at the sea surface (e.g., Holzer and Hall, 2000) and, as discussed in the Introduction, would be simple to interpret if only a single origin time and place needed to be considered. In a general circulation model, one can calculate the varying components contributing at any given location, and use the resulting fractions to find a true mean age and the full range of contributing arrival times. In observations used alone, as we have seen, the apparent age can be a strongly biassed estimate of the mean age.

Consider a Dirichlet-Heaviside, concentration-step, $C = 1$, applied in the North Atlantic Ocean for a radiocarbon-like tracer. Those results can directly be compared to the previous North Atlantic stable tracer experiment. Siberlin (2010) studied three different radioactive tracers $-^3H$ (tritium, $\lambda^{-1} = 17$ years), ^{91}Nb ($\lambda^{-1} = 950$ years), ^{14}C ($\lambda^{-1} = 8267$ years) – and computed their concentration evolution and ages.[1] In the case of tritium, the half-life is so small that the tracer decays long before reaching the Pacific Ocean. Table 1 displays t_{90} and ages for the three decaying tracers. The smaller is λ, the longer are the equilibrium times and the more the tracer age underestimates t_{90}. Many ages or time-scales can be defined in the ocean, and that the definition depends on the tracer studied and the way one defines the boundary conditions. Fig. 10 shows the calculated radiocarbon age from this same experiment, and which is approximately conventional (see e.g., Matsumoto, 2007, Fig. 1). Our map should be compared to Fig. 10 of WH08 for t_{90}. Ages are the oldest in the Pacific and the youngest in the Atlantic. On the Pacific bottom, they are of the order of ~ 2500 years and on the Atlantic bottom ~ 500 years. Those results are pictorially consistent with the mapped deep radiocarbon ages of Matsumoto (2007), but because of the biases, their interpretation is not so clear. One should also note that tracers such as radiocarbon would enter the ocean globally, and not regionally in the manner e.g. of δ^{18}O or ^{3}H. On the other hand, surface physics *is* spatially highly variable involving ice cover, upwelling, downwelling, convection, mixed-layer properties etc., leading to the observed differences in surface

[1] All these tracers are "radiocarbon (etc.)-like" because they are all idealized calculations, lacking e.g., particulate fluxes, the real complexities of the boundary conditions, and biological interactions.

Table 1. Time to near-equilibrium t_{90} and approximate mean tracer ages for several decay constants λ written in terms of the half-life. All values are in years. Boundary conditions were Dirichlet-Heaviside ones. The smaller is λ, the longer is the equilibrium time, and the more the tracer age underestimates the time to equilibrium.

	No Decay	$T_{1/2}=5730y$		$T_{1/2}=700y$		$T_{1/2}=12y$	
Region	t_{90}	t_{90}	age	t_{90}	age	t_{90}	age
Atlantic Bottom	1500	1300	580	850	450	90	105
Iberian Margin	1600	1450	650	900	500	90	110
Pacific Bottom	5500	4400	2330	2100	1600	–	–
East. Eq. Pacific	5800	4600	2500	2300	1730	–	–
Cocos Ridge	6200	5100	2850	2600	1920	–	–

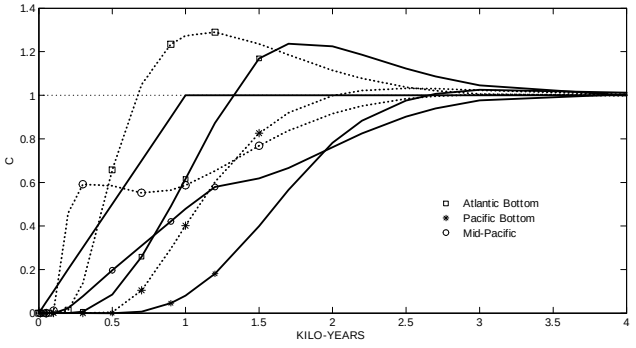

Fig. 8. Neumann-pulse boundary condition applied in the North Pacific: 1000-year pulse (solid lines) and 1-year pulse (dotted lines). Concentration averaged over the global ocean (solid curve without symbols) and at selected areas (bottom of the North Tropical Atlantic, bottom of the North Tropical Pacific and Mid-Pacific) from an injection confined in the North Pacific. Ultimate equilibrium is $C=1$ everywhere.

concentrations, among other features. Thus the physics and routes of entry are likely only going to be understood by picking part the ocean sub-region by sub-region.

The issue of the most appropriate idealized boundary condition is not entirely obvious, although the Robin condition (PD09) is the most natural one, if one can regard the constants appearing there (e.g., the surface diffusion coefficients) as known.[2] Note (e.g., Bard, 1988), that the surface North Atlantic has a radiocarbon age of about 400 years, showing that the ^{14}C concentration there reflects an exchange with the fluid underneath. Ultimately these problems need to be approached by including calculation of the atmospheric concentration as part of the required solution in a coupled system, one in which spatial and temporal variations in upwelling/downwelling and mixing at the base of a time-dependent mixed-layer etc., would be accounted for along with the changing atmospheric concentrations.

[2]Confusingly, the Robin boundary condition, when applied to Helmholtz partial differential equations, is known as a Robbins condition – the terminology used by WH08.

4 Some paleoclimate applications

Studies based on paleodata such as the ones of Skinner and Shackleton (2005) and Lea et al. (2000), using radiocarbon ages, are two examples of attempts to describe the last deglaciation on a regional scale. Between the Atlantic and Pacific bottom however, we calculate here t_{90} from 500 to 4000 years, with a mean value of $\sim$1300 years. No major differences in concentration are observed between the boundaries and the centers of the abyssal basins. From the present results, the glacio-eustatic signal resulting from a pulse-like deglaciation should appear in the cores with t_{90} differences between the Pacific and Atlantic abysses of hundreds to thousands of years, and have undergone significant temporal distortion before being recorded as transients in the two basins.

Furthermore, the temperature of those deep water masses depends essentially on their condition of formation, that is, on the temperature in the area of convection. If we consider sufficiently small changes, the density shift will be so small that temperature is expected to behave as a passive tracer. Large shifts in temperature will change the flow and cannot be treated as a passive tracer. How equilibrium times are changed can only be understood by carrying out a full calculation – not attempted here.

Another example of the use of time delay information is in the core discussed by Lea et al. (2000) in the eastern tropical Pacific near the Galapagos chain. From a passive tracer flux-pulse applied in the North Atlantic, the time required for the sub-surface (0 to 500 m) disturbance in the eastern equatorial Pacific to reach t_{90} exceeds 1500 years although atmospheric pathways require timescales that are far shorter. The fraction of δ^{18}O seen near-surface at the Galapagos owing to a water pathway, as opposed to an atmospheric one, is unknown. Lea et al. (2000) infer a lag of approximately 3 kyrs between the Mg/Ca (primarily a temperature signal) and the δ^{18}O (primarily an ice volume signal) in the planktonic foraminifera in the core, and interpret that to mean that the sea-surface temperature change in the eastern equatorial Pacific led the ice-sheet melting. Furthermore, Lea et al. (2000) conclude that their eastern equatorial SST record is synchronous with the Petit et al. (1999) temperature records

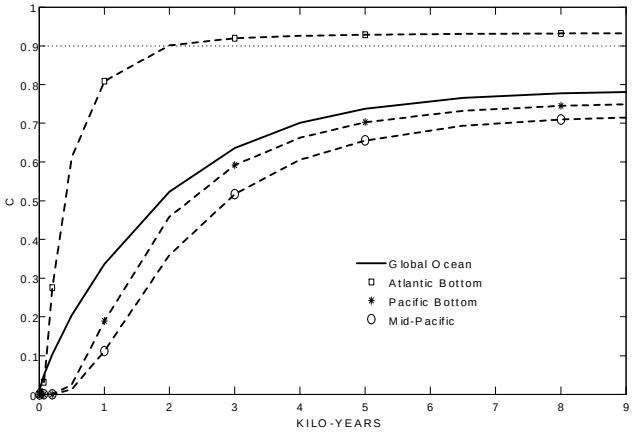

Fig. 9. Concentration from a Dirichlet boundary condition for a radioactive tracer (radiocarbon). Averaged over the global ocean and at selected areas (bottom of the north tropical Atlantic, bottom of the north tropical Pacific and mid-Pacific) from an injection confined to the North Atlantic.

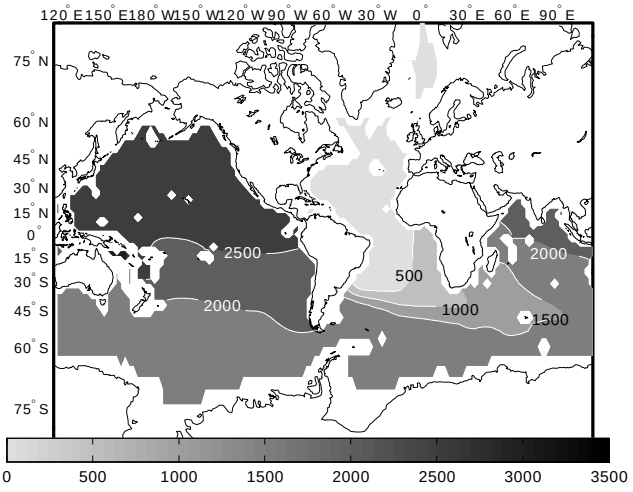

Fig. 10. The radiocarbon age at 2000 m from a North Atlantic Dirichlet-Heaviside input.

in Antarctica "within the 2-ky resolution of the sites." But the ice volume δ^{18}O tracer may have taken several thousand years to reach the core region via the oceanic pathway. Furthermore, in the modern world, high latitude warming is much larger than in the tropics (e.g., IPCC, 2007), and one might anticipate that the lower latitude response will be relatively muted, and delayed. Thus the extent to which causal relationships are truly distinguishable in these and other records needs to be carefully re-examined.

5 Discussion

The purpose of this paper has been to acquire some order of magnitude understanding of the time scales over which tracers move through the global ocean, and the ways in which transients are transformed along the way. In some cases, the approach to near-equilibrium distributions can take many thousands of years and the regional temporal behaviors can be radically different. Removal by diffusion of short time and space scales as pulses move around the ocean can, in particular, greatly change the visual shape of the recorded transients. In many cases, equilibrium times differ by large factors from the commonly used tracer ages.

The matrix method developed by Khatiwala et al. (2005) permits fast computation of the steady and transient states for passive tracers, in which the results are qualtitatively consistent with those obtained by direct integration of the full underlying GCM. Consistent with the results of both WH08 and PD09, the time histories of transient tracers within the ocean have a complex behavior dependent upon the details of the boundary conditions, including not only where and how the tracer is input (Dirichlet, Neumann, or mixed boundary conditions), but also the duration (and area) of a pulse relative to the many internal time scales of tracer movement.

In particular, the time differences required for two oceanic areas to reach a certain concentration depends on those details. If chronologies in cores are set by matching peaks in the local signals and interpreted as representing at least a momentary equilibrium, one must also be alert to the differing nature of the transient approach to equilibrium, most apparent e.g., in the Neumann-pulse cases, where the values may be approached from above in the near-injection region. In many cases not specifically addressed here, the surface boundary conditions may well have changed long before equilibrium is reached in the entire ocean. Temporal structures recorded in different parts of the oceans, even though generated by a common surface boundary condition, may be very different. In contrast, in other cases, time differences of several thousand years may be irrelevant – because they are indistinguishable in the data.

The information content of tracers is not, of course, limited to a reduction to either "age" or equilibrium times. Spatial and temporal gradients at any given time provide information, or at least bounds, on the different terms in equations such as (1) and these could prove fruitful, depending upon the errors introduced by terms that cannot be measured. Similarly, multiple tracers, if imposed with known boundary conditions with adequate accuracy in both space and time, can potentially produce useful bounding values of various oceanic processes.

Boundary conditions

PD09 and F. Primeau and E. Deleersjinder (private communication, 2010) have emphasized the important influence that the choice of boundary condition can make on the resulting time histories. We do not wish here to over-emphasize the direct relevance of our use of a Dirichlet (concentration)

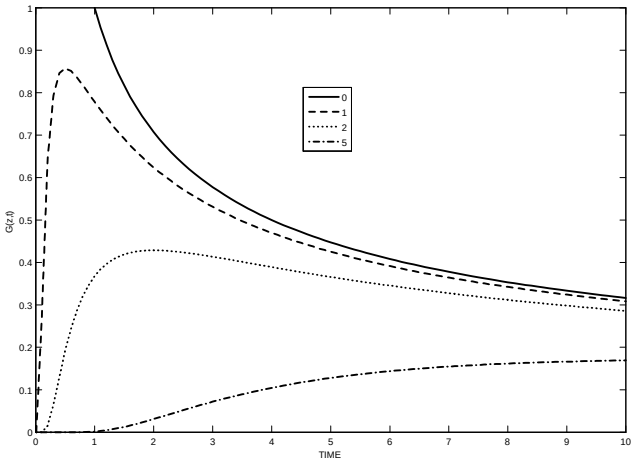

Fig. 11. Boundary Green function for a one-dimensional diffusion problem, showing how a pulse becomes distorted into a slowly rising smooth field. The reduction in the magnitude of C with time and distance occurs because of the mixing with zero concentration fluid in an open system. Different lines are different depths. Units here are arbitrary ones.

surface boundary condition, but regard it as producing, in the geophysical fluid dynamics sense, possibly the simplest method for delineating the internal space-time structures induced by a three-dimensional ocean circulation. Readers need to keep in mind that the evolution of a tracer, and its interpretation, do depend both qualitatively and quantitatively on the details of mechanical injection versus diffusion, gas exchange, precipitation, evaporation, as well as the space and time changes that are inevitable, including seasonality, none of which are discussed here. Parts of the upper ocean undergo convection, some have strong seasonal cycles, some are regions of Ekman suction, and others of Ekman pumping, some are subject to powerful eddy transports, and tracer entry below the surface layers will in practice be regionally a very inhomogeneous process only partially captured here.

For paleoclimate studies, the most important inference is that the tracer is far from being instantaneously homogenized, with times to near-equilibrium extending for thousands of years, and differing sometimes greatly from radiocarbon ages – being usually longer. Ages determined from decaying isotope measurements are biassed to be younger than true mean ages or equilibrium times.

Model limitations

Any study based on GCM results should be considered with care, because of the physics that are either missing or poorly represented, and the present study is no exception. Many limitations exist in these calculations: the major issue being the coarse model spatial resolution. The long-term behavior of so-called eddy-resolving models of the ocean circulation could be very different than the coarse resolution ones used in climate studies (see e.g., Hecht and Smith, 2008; Hecht, 2010; Lévy et al., 2010).

In this model configuration, no "real" ice is formed. The increase of surface water density is the consequence of the low winter temperatures only. Input of freshwater from melting ice at the edges is not represented, nor is the physics of the complex mixed-layer known to be present. When using the 1° horizontal resolution, 21-vertical layer configuration of the ECCO-GODAE-modified-version of the MITgcm (Marshall et al., 1997), WH08, noted some evidence that the model has too-active convection in the North Atlantic; this phenomenon will artificially shorten tracer movement times. On the other hand, when tracer injections occur in regions of AABW formation, we are most likely overestimating the equilibrium times (and those experiments are not described here). Production of AABW depends upon small scale processes taking place on the continental margin and involving complex topography, ice shelves, sea ice, and fine details of the equation-of -state. As a result, the AABW formation is not correctly represented in this (or any other existing) model, with the North Atlantic region dominating the dye concentration of the deepest model layers (WH08). Coarse resolution also prevents an adequate representation of major surface current systems such as the Gulf Stream. Parameterization of the higher resolution features, such as eddies, prevents accurate transport of the dye, especially on the boundaries. With higher resolution, the model would produce higher speed flows and the dye would be advected faster from one point of the ocean to the other. On the other hand, higher resolution also weakens the implicit diffusion existing through the advection scheme, and which would slow the approach to equilibrium. Even if seasonal cycles are present in the underlying GCM code, the use of annual averages of the transition matrices also affects the results. In addition, the vertical diffusion coefficients used in the underlying GCM are uniform and equal to $0.5\,\mathrm{cm}^2\,\mathrm{s}^{-1}$. This value is too high for the thermocline, where $0.1\,\mathrm{cm}^2\,\mathrm{s}^{-1}$ for the diapycnal diffusivity of the upper ocean is more realistic (e.g., Ledwell et al., 1993). Diffusion processes generally determine the time to final approach to an equilibrium state. Further uncertainties would arise, in practice, from the very incomplete knowledge one is likely to have of the time-dependent proxy boundary conditions at the surface.

Active tracers

Apart from the problem of model resolution, probably the greatest limitation on the present study is its restriction to passive tracers – those not affecting the density field – because a state-transition matrix method is not available for the situation where the flow field is changed by the presence of tracer. Although tracers such as δ^{18}O are themselves passive, they are associated with anomalous temperature or salinities in the water carrying them, and hence they are part of an active response. Whether a simple generalization can be

made – that active processes will shorten or lengthen the passive tracer response times – is not obvious. Anomalous density fields can increase or decrease active pressure gradients and hence flows, but they are also subject to confinement by strong rotational constraints, thus slowing the response.

Very preliminary results for an active tracer using direct integration of a 2°-grid resolution global circulation model limited to the North Atlantic box (Siberlin, 2010) showed no significant differences between a small injection of freshwater (0.001 Sverdrups) and of passive dye within the first 50 years of the experiments: the pathways as well as the times required for a change in salinity versus dye concentration are similar. However, any small differences in this critical period could lead to strong differences in the far future as pathways diverge with time. The modern ocean is different from the oceans of the past. At some future time, it will be worthwhile attempting a more detailed estimate of the paleocean circulation.

6 Final remarks

The main outcome here is to raise warning flags about various aspects of proxies recorded in deep ocean sediments. Lead-lag times of apparent shifts in climate record features shorter than about 5000 years need to be viewed cautiously. Radiocarbon ages are particularly problematic when used for causality inferences because of their bias toward younger times. Aside from the usual age-model uncertainties, the ocean all by itself is capable of producing temporal offsets simply through its long adjustment times, as well as qualitative changes in pulse shapes with propagation through the ocean, and which are the result of fully three-dimensional processes. Identifying a particular transient change in one part of the ocean with that perceived in another can be difficult to the point of impossibility. Thus the signal propagation from e.g., the surface North Pacific to the abyssal or intermediate depth North Pacific, is a long and circuitous route not immediately related to the apparently short vertical distance involved. At the present time, for these lead-lag times, there appears to be little alternative except to carry out model integrations through the circulation that are as realistic as possible. Even though the details are unlikely to survive further developments, the gross propagation times and degree of transient distortions should prove robust features of the circulation.

Appendix A

Model configuration

The model and boundary conditions

Surface temperature and salinity are weakly restored to a climatology (Levitus et al., 1998). The configuration uses a third-order direct space time advection scheme ("DST3", linear) with operator splitting for tracers, and a variety of parameterizations to represent unresolved processes, including the Gent and McWilliams (1990) eddy-flux parameterization and the Large et al. (1994) mixed layer formulation (or "KPP"). $\mathbf{A_e}$ and $\mathbf{A_i}$ (the explicit and implicit transport matrices) are derived at monthly resolution from the equilibrium state of the model after 5000 years of integration (Khatiwala, 2007).

In some sub-region, B_1, whose area is all, or a fraction, of B, the boundary condition on C is imposed. WH08 carried out a series of experiments in which the so-called ECCO-GODAE solution v2.216 was used in a perpetual 14-year loop, specifying both $\mathbf{v}$ and $\mathbf{K}$. $\mathbf{v}$ was determined from a least-squares fit of the GCM to a modern data base consisting of over 2×10^9 observations, and thus was believed to be realistic up to the various model approximations (of which the 1° spatial resolution is believed to be the most limiting). Initially, there is no tracer within the model ocean. For boundary conditions on C, WH08 imposed

$$C_{bdy}(\mathbf{r}\in B_1,t)=1H(t), \tag{A1a}$$

$$\frac{\partial C_{bdy}(\mathbf{r}\notin B_1,t)}{\partial z}=0 \tag{A1b}$$

where $H(t)$ is the Heaviside function, $H(t)=0, t<0$; $H(t)=1, t\geq 1$. $\mathbf{r}$ is a three-dimensional position vector. Or, in words, at $t=0$, the concentration at the sea surface in the sub-region B_1 was abruptly set to unity, and maintained at that value ever after. Outside the subregion (if any), the flux into or out of the ocean was set to zero. This particular choice of boundary conditions was made because it permits one to infer the final, asymptotic steady state: $C(\mathbf{r},t\rightarrow\infty)=1$.

Appendix B

Pulse distortion

Diffusion distortion

The simplest system with diffusion is the one-dimensional equation,

$$\frac{\partial C}{\partial t}=K\frac{\partial^2 C}{\partial z^2},$$

with the intitial $C(z,t=0)=0$. At the top boundary, $C_0(t)=\delta(t)$, a pure pulse. The solution to the above equation is then the boundary Green function,

$$G(z,t)=\frac{1}{\sqrt{\pi}}\frac{e^{-z^2/4t}}{\sqrt{t}},$$

in distance units of L, and time units of L^2/K. The result for several values of $-z$ is shown in Fig. 11. A "core" recording the time change at $z=1$, might lead one to infer that the

same event did not occur at $z = 5$. This one-dimensional example mimics the gross behavior of the change in behavior seen over large distances in the GCM results. An elementary analysis, not displayed here, would show that movement through time and space preferentially suppresses short time and space scales, removing the frequencies and wavenumbers necessary to maintain a step-like transient.

Acknowledgements. Supported in part by the National Science Foundation Grant OCE-0824783 and NASA Award NNX08AF09G. The advice and help of S. Khatiwala and of P. Heimbach were essential to this study. P. Huybers, J. Gebbie, S. Khatiwala, F. Primeau and E. Deleersnijder, the two anonymous reviewers, and L. Skinner made several very useful suggestions.

Edited by: L. Skinner

References

Bard, E.: Correction of accelerator mass spectrometry 14C ages measured in planktonic foraminifera: Paleoceanographic implications, Paleoceanog., 3, 635–645, 1988.

Brogan, W.: Modern Control Theory. Third Ed., Prentice-Hall, Englewood Cliffs, NJ, 653 pp., 1991.

Gebbie, G. and. P. Huybers.: How is the ocean filled?, available at: http://www.people.fas.harvard.edu/~phuybers/Doc/filling.pdf, submitted, 2010a.

Gebbie, G., P. Huybers: What is the mean age of the ocean? Accounting for mixing histories in the interpretation of radiocarbon observations, available at:http://www.people.fas.harvard.edu/~phuybers/Doc/radiocarbon_draft.pdf, unpublished ms., 2010b.

Gent, P. R., and Mcwilliams, J. C.: Isopycnal mixing in ocean circulation models, J. Phys. Oc., 20, 150–155, 1990.

Hecht, M. W.: Cautionary tales of persistent accumulation of numerical error: Dispersive centered advection, Ocean Model., 35, 270–276, 2010.

Hecht, M. W. and Smith, R. D.: Towards a physical understanding of the North Atlantic: a review of model studies, in Ocean Modeling in an Eddying Regime, AGU Geophys. Monog. 177, edited by: Hecht, M. W. and Hasumi, H., 213–240, 2008.

Holzer, M. and Hall, T. M.: Transit-time and tracer-age distributions in geophysical flows, J. Atm. Scis. 57, 3539–3558, 2000.

IPCC (Intergovernmental Panel on Climate Change): Climate Change 2007 – The Physical Science Basis, Cambridge Un. Press, Cambridge, 1009 pp., 2007

Jenkins, W. J.: Tritium and helium-3 in the Sargasso Sea. J. Mar. Res., 38, 533–569, 1980

Khatiwala, S., Visbeck, M., and Schlosser, P.: Age tracers in an ocean GCM, Deep-Sea Res. Part I, 48, 1423–1441, 2001.

Khatiwala, S., Visbeck, M., and Cane, M. A.: Accelerated simulation of passive tracers in ocean circulation models, Ocean Modelling, 9, 51–69, doi:10.1016/j.ocemod.2004.04.002, 2005.

Khatiwala, S.: A computational framework for simulation of biogeochemical tracers in the ocean, Global Biogeochem. Cy., 21, Gb3001, doi:10.1029/2007gb002923, 2007.

Large, W. G., Mcwilliams, J. C., and Doney, S. C.: Oceanic vertical mixing – a review and a model with a nonlocal boundary-layer parameterization, Rev. Geophys., 32, 363–403, 1994.

Lea, D. W., Pak, D. K., and Spero, H. J.: Climate impact of late Quaternary equatorial Pacific sea surface temperature variations, Science, 289, 1719–1724, 2000.

Ledwell, J. R., Watson, A. J., and Law, C. S.: Evidence for slow mixing across the pycnocline from an open-ocean tracer-release experiment, Nature, 364, 701–703, 1993.

Boyer, T. P., Conkright, M. E., OBrien, T., Antonov, J., Stephens, C., Stathoplos, L., Johnson, D., and Gelfeld, R.: World Ocean Database 1998,. NOAA Atlas NESDIS 18, NOAA, Silver Spring MD, 1998.

Lévy, M., Klein, P., Treguier, A. M., Iovino, D., Madec, G., Masson, S., and Takahashi, K.: Modifications of gyre circulation by sub-mesoscale physics, Ocean Modelling, 34, 1–15, doi10.1016/j.ocemod.2010.04.001, 2010.

Marshall, J., Adcroft, A., Hill, C., Perelman, L., and Heisey, C.: A finite-volume, incompressible Navier Stokes model for studies of the ocean on parallel computers, J. Geophys. Res.-Oceans, 102, 5753–5766, 1997.

Matsumoto, K.: Radiocarbon-based circulation age of the world oceans, J. Geophys. Res-Oceans, 112, C09004, doi10.1029/2007jc004095, 2007.

Petit, J. R., Jouzel, J., Raynaud, D., Barkov, N. I., Barnola, J. M., Basile, I., Bender, M., Chappellaz, J., Davis, M., Delaygue, G., Delmotte, M., Kotlyakov, V. M., Legrand, M., Lipenkov, V. Y., Lorius, C., Pepin, L., Ritz, C., Saltzman, E., and Stievenard, M.: Climate and atmospheric history of the past 420 000 years from the Vostok ice core, Antarctica, Nature, 399, 429–436, 1999.

Primeau, F. and Deleersnijder, E.: On the time to tracer equilibrium in the global ocean, Ocean. Sci., 5, 13–28, 2009.

Siberlin, C.: Time-Scales of Passive Tracers in the Ocean with Paleoapplications, Master's thesis, Massachusetts Institute of Technology, 134 pp., 2010.

Skinner, L. C. and Shackleton, N. J.: An Atlantic lead over Pacific deep-water change across Termination I: implications for the application of the marine isotope stage stratigraphy, Quat. Sci. Rev., 24, 571–580, doi10.1016/j.quascirev.2004.11.008, 2005.

Waugh, D. W., Vollmer, M. K., Weiss, R. F., Haine, T. W. N., and Hall, T. M.: Transit time distributions in Lake Issyk-Kul, Geophysical Research Letters, 29(223), 2231, doi10.1029/2002gl016201, 2002.

Waugh, D. W., Hall, T. M., and Haine, T. W. N.: Relationships among tracer ages, J. Geophys. Res.-Oceans, 108, 3138, doi10.1029/2002jc001325, 2003.

Wunsch, C.: Oceanic age and transient tracers: Analytical and numerical solutions, J. Geophys. Res.-Oceans, 107, 3048, doi10.1029/2001jc000797, 2002.

Wunsch, C.: Discrete Inverse and State Estimation Problems: With Geophysical Fluid Applications, Cambridge University Press, Cambridge; New York, xi, 371 pp., 2006.

Wunsch, C. and Heimbach, P.: How long to oceanic tracer and proxy equilibrium?, Quat. Sci. Rev., 27, 637–651, 2008.